Wandale and Ichige *EURASIP Journal on Advances in Signal Processing* (2021) 2021:17
https://doi.org/10.1186/s13634-021-00727-5

EURASIP Journal on Advances in Signal Processing

RESEARCH Open Access

Design of sparse arrays via deep learning for enhanced DOA estimation

Steven Wandale and Koichi Ichige*

*Correspondence: koichi@ynu.ac.jp
Department of Electrical and Computer Engineering, Yokohama National University, 79-5 Tokiwadai, Hodogaya-ku, 240-8501, Yokohama, Japan

Abstract

This paper introduces an enhanced deep learning-based (DL) antenna selection approach for optimum sparse linear array selection for direction-of-arrival (DOA) estimation applications. Generally, the antenna selection problem yields a combination of subarrays as a solution. Previous DL-based methods designated these subarrays as classes to fit the problem into a classification problem to which a convolutional neural network (CNN) is employed to solve it. However, these methods sample the combination set randomly to reduce computational cost related to the generation of training data, and it often leads to sub-optimal solutions due to ill-sampling issues. Hence, in this paper, we propose an improved DL-based method by constraining the combination set to retain the hole-free subarrays to enhance the method's performance and sparse subarrays rendered. Numerical examples show that the proposed method yields sparser subarrays with better beampattern properties and improved DOA estimation performance than conventional DL techniques.

Keywords: Antenna selection, Direction-of-arrival estimation, Deep learning

1 Introduction

The design of sparse or non-uniform arrays for DOA estimation-based applications has received tremendous attention due to their ability to resolve $\mathcal{O}(M^2)$ sources given M sensors only. One of the well-known techniques for realizing sparse arrays for DOA estimation applications is array thinning or antenna selection [1–3]. Conventionally, the antenna selection problem is cast as either optimum placement of a given number of antenna elements or selecting an optimum subset of antennas or subarray [4]. Regardless of the formulation, it has been reported in [4–6] that an optimum subarray can preserve a large physical aperture and enables high angular resolution of target localization. Moreover, it reduces the energy and computation costs exerted otherwise on the radio-frequency (RF) system front-end [7–9]. Despite the merits, the art of selecting an optimum subarray from a uniform array is not a trivial matter, and it requires careful consideration of the selection technique depending on the choice of the selection criteria [4–11].

The traditional formulation of antenna selection involves either combinatorial or convex optimization problem formulations. As such, convex relaxation and combinatorial

optimization algorithms are used to obtain optimum subarray while minimizing or maximizing a specific objective function [4–8]. However, such methods involve search-based, and greedy-based algorithms, which are computationally expensive [7]. Learning-based optimization techniques have recently been adopted to solve optimization problems such as antenna selection due to less computationally complex solutions than their conventional counterparts [9–11]. For instance, a support vector machine (SVM) together with an artificial neural network (ANN) was introduced in [9] to realize sparse array configurations that maximize signal-to-interference-plus-noise ratio (SINR) using sensing environmental features extracted from capon-beamformer.

Moreover, [10] proposed a deep learning-based (DL) sparse array selection technique to realize sparse arrays given sample covariance matrix as an input. The method in [10] utilizes a convolutional neural network (CNN) model to predict the best subarray sensor indices, which minimizes the Cramér-Rao bound (CRB) of DOA estimation. In particular, [10] focused on a single source DOA estimation problem on both 1-dimensional (1D) and 2-dimensional (2D) arrays. The approach was extended to multiple sources problems in [11]. Moreover, [11] presents further results on the DOA estimation performance of the rendered sparse arrays using two distinctive DOA estimation methods: the fast iterative soft-thresholding algorithm (FISTA) [12] and multiple signal classification algorithm (MUSIC) [13].

The simulation results in [10] show that the proposed DL-based selector yields suboptimal 1D sparse subarray compared to 2D random and circular subarrays. The realized 1D sparse subarray has sensors located at the end of each side of the uniform linear array (ULA) grid. It was observed in [9] that there is a trade-off between the distribution of sensors in a sparse array and the size of the peak sidelobe levels (PSL), which dictates the variance of DOA estimation. Thus, the linear sparse subarray realized in [10] exhibits high PSLs, hence the poor DOA estimation performance. In this work, we aim to take advantage of the less computation complexity of DL-based algorithms and consider properties of non-uniform sparse linear arrays that control sparse arrays' performance to improve the DL-based selector and corresponding sparse linear arrays.

In this paper, we introduce an enhanced DL-based antenna selection approach. The proposed approach takes advantage of beampattern properties of sparse arrays with a near hole-free or hole-free difference coarray and its impact on peak sidelobe levels and variance DOA estimates. Since picking M antennas out of N-element ULA yields ${}_N\mathrm{C}_M$ possible subarrays, which are considered classes and form the training samples for DL-based selector, we constrain such subarrays to retain a hole-free difference coarray, and the resulting subarrays are used to generate the training dataset. A basic CNN model is employed to classify sparse arrays, which minimize CRB of DOA estimation using the realized dataset. Numerical examples show that the proposed method yields sparser arrays with improved beampattern properties and DOA estimation performance compared to the original large ULA and other well-known sparse arrays.

Notations Throughout the paper, we use lowercase and uppercase bold characters to denote vectors and matrices, respectively, i.e., $\boldsymbol{I}_K$ represents the $K \times K$ identity matrix. Operators $(\cdot)^T$ and $(\cdot)^H$ stand for transpose and the conjugate transpose of a vector or matrix in that order. And vec$(\cdot)$ denotes vectorization operator, and diag$(\cdot)$ represents a diagonal matrix. Moreover, $\odot$ and $E[\cdot]$ denote the Khatri-Rao product and statistical

expectation operator respectively. The calligraphic letter $\mathcal{Z}_i$ denotes a position set of ith array whereas $\boldsymbol{\mathcal{G}}$ and $\boldsymbol{\mathcal{L}}$ consist of all subarrays and optimized subarrays in that order. Moreover, the cardinalities of set $\boldsymbol{\mathcal{G}}$ and $\boldsymbol{\mathcal{L}}$ are given by non-bold capital letters G and L for $|\boldsymbol{\mathcal{G}}|$ and $|\boldsymbol{\mathcal{L}}|$, respectively. The operator ${}_{(\cdot)}\mathrm{C}_{(\cdot)}$ represents combination whereas functions $\angle\{\cdot\}$, $\mathbb{R}\mathrm{e}\{\cdot\}$ and $\mathbb{I}\mathrm{m}\{\cdot\}$ indicate the phase, real and imaginary parts of a complex argument in that order.

2 Preliminaries

Consider a ULA with N sensors with interelement spacing of $z_n a_o, z_n \in \mathcal{Z}$ for $n = 1, 2, \ldots, N$ where $\mathcal{Z}$ denotes the set of sensor positions of the physical array. Assuming that D uncorrelated narrowband sources are impinging on the array from far field directions $\theta_1, \theta_2, ..., \theta_d$, for $d = 1, 2, ..., D$. Then, the dth source steering vector can be expressed as

$$\boldsymbol{a}(\theta_d) = \left[1, e^{jz_2 a_o \kappa \sin(\theta_d)}, \ldots, e^{jz_M a_o \kappa \sin(\theta_d)}\right]^T, \tag{1}$$

where $\kappa = 2\pi/\lambda$, $a_o = 1/\lambda$ and λ is the carrier's frequency wavelength. As such, the received signal vector can be expressed as

$$\boldsymbol{x}(t) = \boldsymbol{A}\boldsymbol{s}(t) + \boldsymbol{n}(t), \tag{2}$$

where $\boldsymbol{s}(t)$ and $\boldsymbol{n}(t)$ are the source signal vector and the noise vector at tth snapshot. respectively. And, $\boldsymbol{A} = [\boldsymbol{a}(\theta_1), \boldsymbol{a}(\theta_2), \ldots, \boldsymbol{a}(\theta_D)]$ is the array steering matrix. Moreover, the noise is assumed to be additive white Gaussian noise (AWGN) and that the source signals and the noise are uncorrelated [14–16]. Thus, the corresponding covariance matrix of $\boldsymbol{x}(t)$ can be expressed as

$$\boldsymbol{R}_x = E\left[\boldsymbol{x}(t)\boldsymbol{x}^H(t)\right] = \boldsymbol{A}\boldsymbol{R}_s\boldsymbol{A}^H + \sigma_n^2\boldsymbol{I}_N, \tag{3}$$

where $\boldsymbol{R}_s = \mathrm{diag}(\rho_1, \rho_2, \ldots, \rho_D)$ is the signal covariance matrix such that ρ_i for $i = 1, 2, \ldots, D$ denote the signal power powers, and σ_n^2 denotes additive noise power. Following [17–21], vectorizing (3) yields

$$\boldsymbol{y} = \mathrm{vec}(\boldsymbol{R}_x) = \boldsymbol{B}_c\boldsymbol{p} + \sigma_n^2\mathrm{vec}(\boldsymbol{I}_N), \tag{4}$$

where $\boldsymbol{B}_c = (\boldsymbol{A}^* \odot \boldsymbol{A})$, $\boldsymbol{p}$ is the source signal and $\boldsymbol{y}$ becomes the new received signal vector based on coarray model [17]. Note that $\boldsymbol{B}_c$ denotes the new steering matrix of the coarray model whose sensor locations are defined as a difference between the sensor positions of $\mathcal{Z}$ i.e., $\mathcal{Q}_u = \{n_1 - n_2 | n_1, n_2 \in \mathcal{Z}\}$ [18]. Cleaning-off duplicate components of $\boldsymbol{B}_c$ yields an extended steering matrix denoting a virtual ULA of size $\mathcal{O}(N^2)$ given N sensors. As a result, applying a coarray based DOA estimator, i.e., coarray MUSIC, on (4), it is possible to estimate more sources than number of sensors [17, 19].

Note that the unique element in set $\mathcal{Q}_u$ is defined as difference coarray $\mathcal{Q}$. Thus, the number that element or lag $q (q \in \mathcal{Q}_u)$ occurs in set $\mathcal{Q}$ is known as weight function $w(q)$. If $w(q_1) > 1$ then q_1 is a redundant lag (R). Else, if $w(q_1) = 0$, then the coarray has a hole (H) or missing sensor at lag q_1. Figure 1 illustrates the coarray properties of a typical sparse array $\mathcal{Z} = [0, 1, 2, 6]$. From Fig. 1a, the central contiguous segment of sensors is termed the central ULA segment ($\mathbb{U}$). Furthermore, if the holes does not exist in the coarray, then the coarray retains a large $\mathbb{U}$. Otherwise, the coarray size shrinks [17–20].

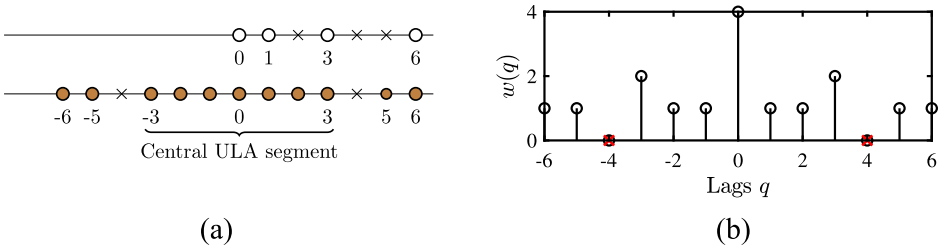

Fig. 1 Coarray properties of a sparse linear array $\mathcal{Z}$. **a** The physical array $\mathcal{Z}$ (top) and difference coarray (bottom). **b** A weight function of sparse array $\mathcal{Z}$. The circles denote physical sensors, the filled circle denotes a virtual sensor and the cross represents a missing sensor or hole

3 Methods

This section introduces the methods used in work. Antenna selection problem formulation is introduced first, followed by a review of the relationship between coarray, sparse arrays, and minimum sidelobe level. This is followed by the proposed approach, corresponding training data generation procedures, and the CNN structure.

3.1 Antenna selection problem formulation

Given a ULA with N elements, the number of possible combinations M elements can be picked from the ULA is defined as [7]

$$G = {}_N\mathrm{C}_M = \frac{N!}{M!\,(N-M)!}. \tag{5}$$

As in [10], all possible subarrays in (5) are considered as classes. Assuming that set $\mathcal{G}$ contains all classes in (5), and that each $\boldsymbol{g} \in \mathcal{G}$ is associated with x_m and y_m, for $m = 1, \ldots, M$ in xy-plane, then the gth class consisting of all antenna elements in gth subarray can be denoted as $\mathcal{Z}_g = \{z_1^g, z_2^g, \ldots, z_M^g\}$. As a result, $\mathcal{G}$ can be redefined as $\mathcal{G} = \{\mathcal{Z}_1, \mathcal{Z}_2, \ldots, \mathcal{Z}_G\}$ [10]. The assumptions above transform the antenna selection problem from a combinatorial optimization framework to a ML classification framework. Any ML or DL-based classification algorithm can be employed to classify the desired class (subarray) using appropriate metrics that characterize the best class (sparse subarray configuration in our case). However, this is possible if labels for the classes are known [11].

3.2 Coarray, sparse arrays, and minimum sidelobe level

In sparse array processing, it is well-known that for efficient spatial sampling purposes, an array whose coarray has no redundancy or holes is considered as a perfect array [7, 19]. Assuming no holes exist ($H = 0$), a perfect array aperture can be defined as

$$|\mathcal{Z}_a| = \frac{N(N-1)}{2}, \tag{6}$$

where $|\mathcal{Z}_a|$ is the array aperture and N is the number of antennas. Unfortunately, such an array does not exist for $N > 4$ [20]. Alternatively, one can construct a sparse array with no holes but retains the largest possible aperture, i.e., $|\mathcal{Z}_a|$ to approximate the perfect array. Consequently, several methods have been proposed in [7, 19, 20] for designing of minimum redundancy array as well as minimum hole arrays. Here, the former is the array that minimizes $(R|H = 0, N = constant)$ for a given N elements, whereas the latter minimizes holes in the coarray.

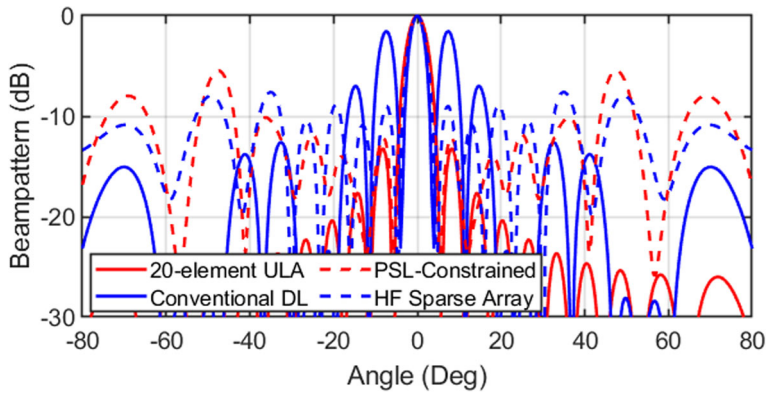

Fig. 2 Beampattern responses of 20—element ULA, 20—element conventional DL array, 20—element PSL-constrained array and 20—element sparse array with a hole-free difference coarray

These arrays are attractive due to their good beampattern properties—PSLs and narrow main lobe [7]. For instance, Fig. 2 compares the beampattern responses of ULA, a conventional DL proposed in [10], PSL-constrained array proposed in [8], and sparse array with a hole-free difference coarray. It can be observed that the beampattern response of conventional DL shows high PSLs as compared to that of PSL-constrained and sparse array with a hole-free difference coarray which shows well suppressed PSLs. Although the relationship between the two concepts is not directly proved here, the connection was thoroughly investigated in [7, 19–21], and sparse array with hole-free coarray or with minimum redundancy and minimum holes were recommended as the best solution for array thinning because of their narrow main lobe and minimum PSLs. Hence, inspired by beampattern properties of MRA and MHA as well as the work in [8], we aim to impose a hole-free constraining term on the solution set $\boldsymbol{\mathcal{G}}$ which is used to create the training dataset in a bid to improve the performance DL-based antenna selection technique.

3.3 Proposed DL-based antenna selection approach

Motivated by beampattern properties of MHAs and MRAs [7], we extend and enhance the DL-based antenna selection technique proposed in [10]. By taking advantage of essential sensor properties of the array as introduced in [19, 20], we constrain the subarrays in the solution set (5) to retain a hole-free difference coarray as a means of enforcing sensor distribution within subarrays that form the feature space.

The idea is given a solution set $\boldsymbol{\mathcal{G}}$ which consists of subarrays as possible solutions to a ${}_{N}\mathrm{C}_{M}$ antenna selection problem. We intend to use all $\boldsymbol{g} \in \boldsymbol{\mathcal{G}}$ which retains a hole-free difference coarray only to generate the training dataset and discard the rest. As a result, we implement a basic search algorithm to search through $\boldsymbol{\mathcal{G}}$ and reserve all $\boldsymbol{g} \in \boldsymbol{\mathcal{G}}$ with a hole-free difference array, i.e., $\mathcal{Q}_g = \mathcal{Q}_{ULA}$ and omit those without, i.e., $\mathcal{Q}_g \neq \mathcal{Q}_{ULA}$ where $\mathcal{Q}_g$ and $\mathcal{Q}_{ULA}$ are difference coarrays of a M- sensor subarray $\boldsymbol{g} \in \boldsymbol{\mathcal{G}}$ and N- sensor ULA respectively. The steps above are summarized in Algorithm 1.

In other words, the difference coarray as a constraint on every $\boldsymbol{g} \in \boldsymbol{\mathcal{G}}$ can be expressed in terms of *essential property of sensors* of an array. For multiple sensors failure or omission, the essential property states that

Algorithm 1 Implemenation of a hole-free difference coarray constraint on $\boldsymbol{\mathcal{G}}$

Input: Total number of sensors N, number of sensors to be selected M.

Output: $\boldsymbol{\mathcal{L}}$

```
Compute 𝒢 using (5)
for g ∈ 𝒢 do
    if 𝒬_g ≠ 𝒬_ULA then
        ℒ ← g.
    end if
end for
return ℒ
```

Property 1 (k-essential property [19]) *$\mathcal{S} \subset \mathcal{Z}$ is said to be k-essential when (1) $|\mathcal{S}| = k$, and (2) the difference coarray changes when $\mathcal{S}$ is removed from $\mathcal{Z}$ i.e. $\hat{\mathcal{Q}} \neq \mathcal{Q}$ where $\hat{\mathcal{Q}}$ and $\mathcal{Q}$ are difference coarrays of $\mathcal{Z}\backslash\mathcal{S}$ and $\mathcal{Z}$ respectively.*

This entails that $N - M$ sensors, which are not essential for the preservation of the N-sensor array's difference coarray, can be discarded out N-sensor array without changing the array aperture and difference coarray. Therefore, we can reformulate the property 1 and define it with respect to the antenna selection problem as follows

Property 2 *Let $\mathcal{Q}$ be the difference coarray of a physical subarray $\mathcal{Z}_g$ such that $\mathcal{Z}_g \triangleq \boldsymbol{g} \in \boldsymbol{\mathcal{G}}$. If $\boldsymbol{\mathcal{G}}$ consists of all possible subarrays as solutions to an (N, M) antenna selection problem, then for all $\boldsymbol{g} \in \boldsymbol{\mathcal{G}}$, $\boldsymbol{g}$ is essential with respect to $\mathcal{Z}_{ULA}$ if the difference coarray of the large array $\mathcal{Z}_N$ changes when $\boldsymbol{g}$ is removed, that is, if $\mathcal{Z}_g = \mathcal{Z}_{ULA}\backslash\boldsymbol{g}$, then $\grave{\mathcal{Q}} \neq \mathcal{Q}$ where $\grave{\mathcal{Q}}$ and $\mathcal{Q}$ are difference coarrays of $\mathcal{Z}_g$ and $\mathcal{Z}_{ULA}$ respectively.*

Note that the use of hole-free subarrays will not only assist in the realization of sparser subarrays with the well-distributed sensors but also sparse arrays with improved beampattern characteristics [7]. As a result, instead of using (5) as in [10] when preparing the training dataset, we resolve to use $\boldsymbol{\mathcal{L}}$, output from Algorithm 1. Henceforth, for clarity sake, we refer to the implementation using $\boldsymbol{\mathcal{L}}$ as the proposed method and the one using $\boldsymbol{\mathcal{G}}$ or a portion of (5) as conventional method [10].

3.4 Training dataset generation for antenna selection problem

In this section, we consider training dataset generation–input data samples and corresponding labels or ground truths. Basically, the feature space is comprised of angle, real and imaginary components of a sample covariance matrix $\hat{\boldsymbol{R}}$. Thus, the input data is $N \times N \times 3$ real-valued matrices $\{\boldsymbol{H}\}_{i=1}^{3}$ whose $(i,j)-$th entry consists of $[\boldsymbol{H}_1]_{i,j} = \angle[\hat{\boldsymbol{R}}]_{i,j}$, $[\boldsymbol{H}_2]_{i,j} = \mathbb{R}\mathrm{e}[\hat{\boldsymbol{R}}]_{i,j}$ and $[\boldsymbol{H}_3]_{i,j} = \mathbb{I}\mathrm{m}[\hat{\boldsymbol{R}}]_{i,j}$ denoting the phase, real and imaginary components of sample covariance matrix $\hat{\boldsymbol{R}}$ [10].

To generate input-out training dataset pairs, we need to determine subarrays with the best performance within the solution set $\boldsymbol{\mathcal{L}}$ to act as ground truths or labels. For simplicity, like [10], we assume the CRB as a benchmark of determining the best array configurations. Therefore, we assume that the received signal vector at lth subarray with M elements is defined as

$$\boldsymbol{x}_l(t) = \boldsymbol{A}_l \boldsymbol{s}_l(t) + \boldsymbol{n}_l(t), \tag{7}$$

where $\boldsymbol{A}_l$ is the subarray steering matrix, $\boldsymbol{s}_l(t)$ denotes the signal vector and $\boldsymbol{n}_l(t)$ is the noise vector corresponding to the lth subarray position set $\mathcal{Z}_l$ at the tth snapshot. Like (2), we assume that $\boldsymbol{s}_l(t)$ and $\boldsymbol{n}_l(t)$ are spatially and temporarily uncorrelated [14, 16]. Furthermore, we assume constant signal variance σ_s^2 and noise variance σ_n^2. Hence, the signal-to-noise ratio (SNR) in dB is expressed as $\text{SNR} = 10\log_{10}\left(\sigma_s^2/\sigma_n^2\right)$.

Therefore, following assumptions in [15], the CRB_θ for every $\boldsymbol{l} \in \boldsymbol{\mathcal{L}}$ can be expressed as

$$\mathcal{C}(\theta, \mathcal{Z}_l) = \frac{\sigma_n^2}{2T}\left[\Re\left\{\left(\boldsymbol{B}^H \boldsymbol{P}_A^{\perp} \boldsymbol{B}\right) \odot \left(\boldsymbol{R}_s \boldsymbol{A}_l^H \boldsymbol{R}_l^{-1} \boldsymbol{A}_l \boldsymbol{R}_s\right)^T\right\}\right]^{-1}, \tag{8}$$

where $\boldsymbol{P}_A^{\perp} = \boldsymbol{I} - \boldsymbol{A}_l\left(\boldsymbol{A}_l^H \boldsymbol{A}_l\right)^{-1}\boldsymbol{A}_l^H$ is the orthogonal projection onto the null space of $\boldsymbol{A}_l^H$, $\boldsymbol{B} = [\boldsymbol{b}(\theta_1), \boldsymbol{b}(\theta_2), \ldots, \boldsymbol{b}(\theta_D)]$ such that $\boldsymbol{b}(\theta_i) = \frac{\partial}{\partial \theta_i}\boldsymbol{A}_l(\theta_i)$ for $i = 1, 2, \ldots, D$ and

$$\boldsymbol{R}_l = E\left[\boldsymbol{x}_l(t)\boldsymbol{x}_l^H(t)\right] = \boldsymbol{A}_l \boldsymbol{R}_s \boldsymbol{A}_l^H + \sigma^2 \boldsymbol{I}_M. \tag{9}$$

Next, for various DOAs, we construct sample covariance matrices $\boldsymbol{R}_l$ for $l = 1, 2, \ldots, L$ and compute CRBs for all $\boldsymbol{l} \in \boldsymbol{\mathcal{L}}$. Then, subarrays with lowest CRBs for various DOAs selected and save into $\boldsymbol{\mathcal{W}}$. Here, $\boldsymbol{w}_i \in \boldsymbol{\mathcal{W}}$ for $i = 1, 2, \ldots, W$ represents class labels such that $\boldsymbol{w}$ is defined as

$$\boldsymbol{w} = \underset{l=1,2,\ldots,L}{\operatorname{argmin}} \mathcal{C}(\theta_d, \mathcal{Z}_l). \tag{10}$$

Following (10) and realization of $\boldsymbol{\mathcal{W}}$, we construct input-output data pairs as $(\boldsymbol{H}, \boldsymbol{w})$ where $\boldsymbol{H}$ is the real-value input data obtained from the covariance matrix and $\boldsymbol{w} \in \boldsymbol{\mathcal{W}}$ is the label representing the best subarrays sensor positions for the sample covariance matrix $\hat{\boldsymbol{R}}$ [10]. The above training dataset generation procedures are summarized in Algorithm 2.

Algorithm 2 Training dataset generation

Input: Total number of given antennas N, number of antennas to be selected M, number of snapshots T, number of different DOA angles D, number of signals and noise realizations Q and $\text{SNR}_{\text{TRAIN}}$

Output: Training data $\boldsymbol{\mathcal{D}}_{\text{TRAIN}}$

1: Compute $\mathcal{G}_l$ using Algorithm 1

2: Generate D_θ DoA angles θ_d for $d = 1, 2, \ldots, D_\theta$.

3: Generate Q different realizations of subarray output, $\left\{\boldsymbol{X}_d^i\right\}_{i=1}^{Q}$ for $d = 1, \ldots, D_\theta$

$$\boldsymbol{X}_d^i = \left[\mathbf{x}_d^i(1), \mathbf{x}_d^i(2), \ldots, \mathbf{x}_d^i(T)\right],$$

where $\mathbf{x}_d^i(t) = \boldsymbol{a}(d)\boldsymbol{s}^{(i)}(t) + \boldsymbol{n}^{(i)}(t), \boldsymbol{s}^{(i)}(t) \sim \mathcal{CN}\left(0, \sigma_s^2 \boldsymbol{I}\right)$ and $\boldsymbol{n}^{(i)}(t) \sim \mathcal{CN}\left(0, \sigma_n^2\right)$

4: Construct sample covariance matrix $\hat{\boldsymbol{R}}$ and $M \times M$ covariance matrices $R_l^{(i,d)}$ for $l = 1, 2, \ldots, L$.

5: Compute CRB values $\mathcal{C}(\theta_d, \mathcal{Z}_l)$ for all $\boldsymbol{l} \in \boldsymbol{\mathcal{L}}$ and select subarrays with the lowest CRB values using (10). Then, construct the set of labels as $\boldsymbol{\mathcal{W}}$.

6: Compute input-output pairs as $\left(\hat{\boldsymbol{R}}^{(i,d)}, w_d^{(i)}\right)$ for $d = 1, \ldots, D_\theta$ and for $i = 1, \ldots, Q$.

7: Calculate the input-output pairs to form the training dataset as

$$\boldsymbol{\mathcal{D}}_{\text{TRAIN}} = \left[\left(\hat{\boldsymbol{R}}^{(1,1)}, w_1^{(1)}\right), \left(\hat{\boldsymbol{R}}^{(2,1)}, w_1^{(2)}\right), \ldots, \left(\hat{\boldsymbol{R}}^{(Q,1)}, w_1^{(Q)}\right), \left(\hat{\boldsymbol{R}}^{(1,2)}, w_2^{(1)}\right), \ldots, \left(R^{(Q,D_\theta)}, w_{D_\theta}^{Q}\right)\right]$$

where the size of the training dataset is $\mathcal{P} = QD_\theta$.

3.5 Convolutional neural network architecture

In this work, we adopt a general CNN structure consisting of 9 sections as in [10]. In general terms, the first layer (1st layer) accepts the 2D input and the last output layer (9th layer) is a classification layer with l units where a softmax function is used to obtain the probability distribution of the classes [22]. The second (2nd layer) and the fourth (4th layer) layers are max-pooling layers with 2×2 kernel to reduce the dimension whereas the third (3rd layer) and the fifth (5th layer) layers are convolutional layers with 64 filters of size 3×3.

Finally, the seventh (7th layer) and the eighth (8th layer) layers are fully connected layers with 1024 units. Note that the rectified linear units (ReLU) are used after each convolutional and fully connected layers such that $\mathrm{ReLU}(x) = \max(x, 0)$ [11]. Furthermore, during the training phase, 90% and 10% of the data are allocated for training and validation purposes, respectively. The stochastic gradient descent with momentum (SGD) is used with a learning rate of 0.03 and a mini-batch of 500 for 50 epochs [10].

4 Results and discussion

In this section, we perform a series of numerical simulations to evaluate the performance of the proposed antenna selection approach as well as the performance of the realized DL-based sparse linear arrays. First, we train our CNN model and predict sparse arrays. This is followed by sparse array performance evaluations in terms of array configuration, beampattern characteristics, and DOA estimation performance.

We measure the DOA estimation performance of the arrays using root-mean-square-error (RMSE), which can be expressed as

$$\mathrm{RMSE} = \sqrt{\frac{1}{DC}\sum_{d=1}^{D}\sum_{c=1}^{C}\left(\hat{\theta}_d^{(c)} - \theta_d^{(c)}\right)^2}, \tag{11}$$

where, $\theta_d^{(c)}$ is the dth DOA in the cth simulation trial, and $\hat{\theta}_d^{(c)}$ is the corresponding angle estimate. Moreover, for performance comparison purposes, we consider the following conventional sparse linear arrays with sensor positions defined as

$$\begin{aligned}
\mathcal{Z}_{\mathrm{DA}} &= [0, 1, 2, 3, 4, 15, 16, 17, 18, 19], \\
\mathcal{Z}_{\mathrm{PSA}} &= [0, 2, 5, 6, 8, 11, 13, 15, 16, 19], \\
\mathcal{Z}_{\mathrm{NA}} &= [0, 1, 2, 3, 7, 11, 15, 19, 23, 27], \\
\mathcal{Z}_{\mathrm{MRA}} &= [0, 1, 4, 10, 16, 22, 28, 33, 35],
\end{aligned}$$

where DA is the conventional DL-based array proposed in [10] for a $(20, 10)$ antenna selection problem, PSA is the PSL-constrained array proposed in [8], $M_1 = 3$ and $M_2 = 7$ nested array [18] and $10-$element MRA [21] in that order. Note that all conventional sparse arrays share the same number of sensors $M = 10$ but differs in aperture sizes.

4.1 Sparse array selection using DL-based method

In this example, we aim to select a $10-$element ($M = 10$) sparse array from a $20-$element ULA ($N = 20$) using the proposed DL-based technique. The problem yields ${}_{20}\mathrm{C}_{10} = 184756$ subarrays ,i.e, $\mathcal{G}$. However, after applying Algorithm 1, the instances dropped to 14791 subarrays ,i.e., $\mathcal{L}$. This is followed by selection of the best subarray to calculate

Table 1 Sample sets versus number of labels for (20, 10) antenna selection problem

Approach	Samples/ classes	Realized labels
Conventional [21]	184756	71
Proposed	1491	67

$\mathcal{W}$, which was found to consists of 67 subarrays for the proposed method and 71 for the conventional method. As pointed out in [9–11], the size of $\mathcal{W}$ is much less as compared to that of $\mathcal{L}$.

Table 1 briefly compares the solution sets against the number of labels realized between the conventional and the proposed methods. A closer look shows that the number of labels generated in each case is comparably the same. This indicates that the proposed method does not only helps to enhance the DL-based antenna selection approach proposed in [10] but also reduces computational load associated with training dataset annotation.

The CNN model as defined in Section (3.5) was trained for $M = 10$, $N = 20$. The training dataset was generated using $\mathrm{SNR}_{\mathrm{TRAIN}} = 10$ dB, $\mathrm{T}_{\mathrm{TRAIN}} = 100$ snapshots, $\mathrm{Q}_{\mathrm{TRAIN}} = 120$ signal, and noise realisation and $(D_\theta)_{TRAIN} = 120$ DOAs spaced uniformly within $\theta \in (-90°, 90°)$. During testing, M, N, and T were kept constant whereas $\mathrm{SNR}_{\mathrm{TEST}} = 0$ dB, $Q = 1$, and $D_\theta)_{TEST} = 2$ DOAs picked randomly in within the same range of $(-90°, 90°)$.

Figure 3 shows the array configurations of the predicted sparse arrays. We observed that the array configurations of the proposed method are as sparse as most conventional sparse arrays. Moreover, the predicted sparse arrays exhibit hole-free difference coarrays identical to the size of the difference coarray of the original 20-element ULA, i.e., $\mathcal{O}(N)$. This large difference coarray $\mathcal{Q}$ enables the predicted sparse arrays to estimate more uncorrelated sources than the number of sensors.

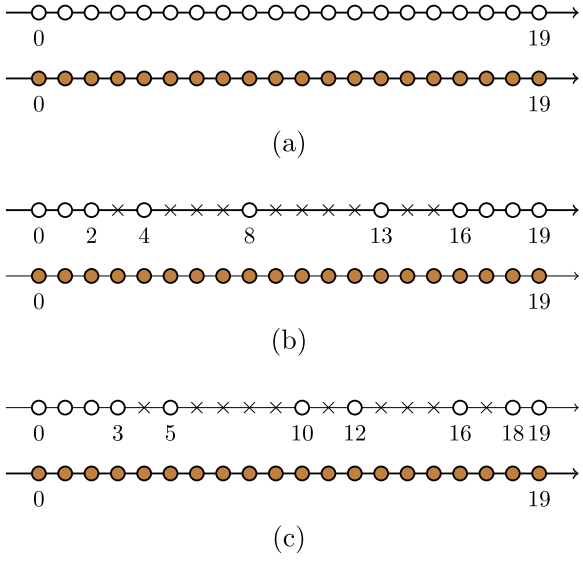

Fig. 3 Predicted sparse array configurations (top) and their corresponding difference coarrays (bottom). Here, **a** original 20-element ULA, **b** proposed 1 and **c** proposed 2. The bullets and the crosses represent physical elements and empty spaces in that order whereas the filled circles denote virtual sensors in the difference coarray

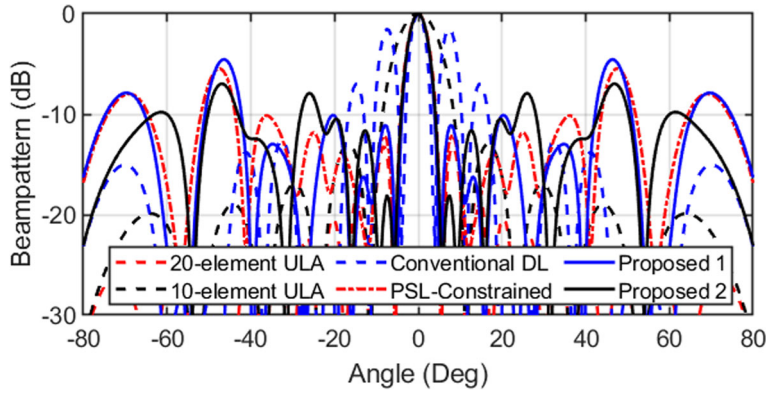

Fig. 4 Beampattern comparison among the 20−element ULA, the 10−elements ULA, the 10−element conventional DL-based array, 10−element PSL-constrained array and the 10−element proposed DL-based array

4.2 Beampattern response of the proposed sparse arrays

In this section, we evaluate the beampattern responses of the proposed DL-based sparse arrays in comparison to the responses of conventional sparse arrays. In the example, the look angle is assumed to be located at $\theta = 0°$. Figure 4 shows the computed beampattern responses.

It can be observed in Fig. 4 that the beampattern response of the conventional DL array shows high PSLs as compared to the PSL-constrained array, which shows well suppressed PSLs. Moreover, the proposed arrays with hole-free difference coarray yield beampatterns with well suppressed PSLs such that the PSLs are closer to that of the PSL-constrained array. This indicates the proposed method's effectiveness in yielding sparse arrays with enhanced beampattern properties [7].

4.3 DOA estimation performance of the proposed sparse arrays

In this section, we examine the DOA estimation performance of the predicted sparse arrays in comparison to conventional DL-based arrays, original 20−element ULA, 10−element ULA, and 10−element PSL-constrained array. We consider $D = 3$ sources case where the sources are uniformly distributed between $[-60°$ to $60°]$, and root-MUSIC estimator is utilized to calculate RMSE as a function of SNR and number of snapshots [12]. In the first scenario, we compute RMSE versus SNR with $D = 3$, 500 snapshots over 1000 trials while varying the SNR from -20 dB to 10 dB. In the second scenario, we compute RMSE versus the number of snapshots with $D = 3$, SNR $= 0$ dB over 1000 trials while varying the number of snapshots from 50 to 600. Figure 5 shows the plot of RMSE versus SNR (left) and RMSE versus number of snapshots (right).

As shown in Fig. 5, the proposed sparse arrays show better performances comparable to PSL-constrained and closer to the performance of the original 20-element ULA throughout the SNR and number of snapshots levels. Moreover, the predicted sparse arrays performed better than 10−element ULA and conventional DL. The results demonstrate that the proposed antenna selection approach can be used to thin or select sparse arrays with few sensors instead of a full array without degrading the estimation accuracy considerably while reducing the computation cost.

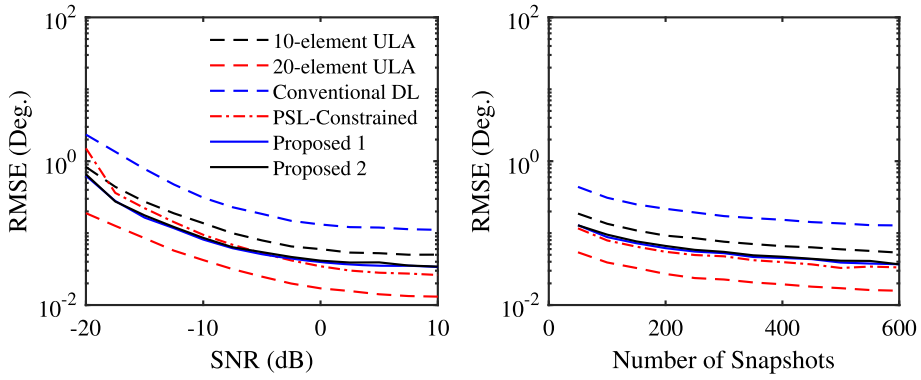

Fig. 5 RMSE performance of the predicted DL-based sparse arrays

4.4 DOA estimation performance comparison with conventional sparse arrays

In this example, we consider DOA estimation of more sources than the number of sensors. Specifically, we compare the performance of the predicted sparse arrays with MRA, NA, and the original 20-element ULA. To that end, we consider $D = 11$ sources case and the RMSE of DOA estimation as a function of SNR and number of snapshots. Like the previous example, we compute RMSE versus SNR with $D = 11$, 1000 snapshots over 500 trials while varying the SNR from -20 dB to 10 dB. Then, we compute RMSE versus the number of snapshots with $D = 11$, SNR $= 0$ dB over 500 trials while varying the number of snapshots from 50 to 500. Note that the sources were assumed to be distributed uniformly between $[-60°, 72°]$. Figure 6 shows the plot of RMSE versus (left) SNR and (right) number of snapshots.

Figure 6 shows that the predicted sparse arrays exhibit better performances slightly higher than the performance of the original 20-element ULA, MRA, and NA but better than the performance of PSL-constrained despite sharing the same size of the aperture. However, the same is not the case with MRA and NA because MRA and NA have large array aperture as compared to the predicted sparse arrays. Nonetheless, the results indicate the potential and the effectiveness of the proposed antenna selection technique.

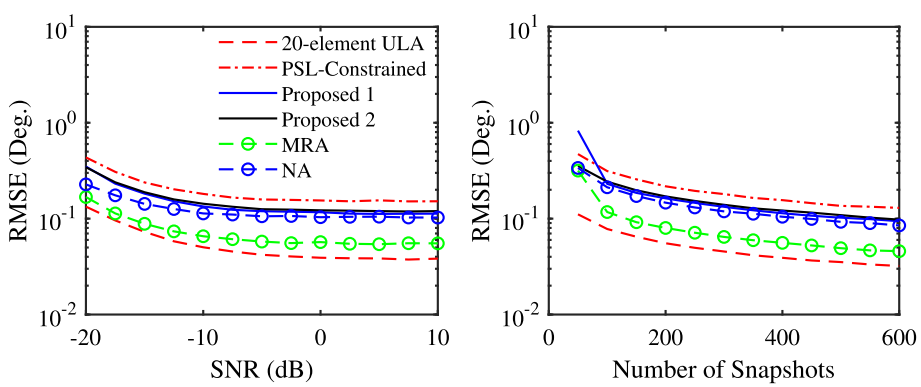

Fig. 6 RMSE performance of the predicted DL-based sparse arrays in comparison to other sparse arrays

4.5 Computation complexity analysis

The time complexity of DL neural network can be approximated using the complexity of the convolutional and fully connected layers as [10, 22]

$$\mathcal{T}_{DL} = \mathcal{O}\left(\sum_{r=1}^{R_{cl}} \mathcal{D}^r v^r \mathcal{J}_{cl}^{r-1} \mathcal{J}_{cl}^r\right) + \mathcal{O}\left(\sum_{r=1}^{R_{fl}} \mathcal{D}^r \mathcal{J}_{fl}^r\right), \tag{12}$$

where for the first term $\mathcal{D}^r$, v^r, $\mathcal{J}_{cl}^{r-1}$, and $\mathcal{J}_{cl}^r$ denote the size of output feature map, 2D filter size, number of input, and output features of the rth convolutional layers, respectively. And for the second term, $\mathcal{D}^r$ and $\mathcal{J}_{fl}^r$ represents the size of 2D input and total number of units of rth fully connected layer, respectively. Assuming 2 convolutional layers with 64 feature maps with 3×3 kernel and 2 fully connected layers, operations with respect to the first and second terms of (12) can be approximated as $\left(N^2 \cdot \left(2 \cdot 9 \cdot 64^2\right)\right)$ and $\left(2 \cdot 64^2 \left(N^2 + 2\right)\right)$ in that order. Thus, combining the two terms yield $\left(64^2 \left(22N^2 + 4\right)\right)$ and the corresponding $\mathcal{T}_{DL}$ is $\mathcal{O}\left(64^2 \left(22N^2 + 4\right)\right)$ which can be further simplified to $\mathcal{O}\left(22 \cdot 64^2 N^2\right)$ [22].

In comparison, the order of a convex relaxation algorithm (through the difference of two convex sets, which is a polynomial-time algorithm) used to design PSL-constrained array in [8] is almost $\mathcal{O}\left(N^3 + N^2 L\right)$. However, once trained, the DL-based selector requires very few matrix computations to yields the best solution. For instance, running the models in MATLAB using a PC with Intel(R) Core (TM)-i5 at 2.60 GHz with 4 GB RAM, the proposed DL-based method required only $0.0270s$ (prediction phase only) to predict a sparse array, whereas the approach in [8] takes almost $0.157s$ for $N = 20$ and $M = 10$ case.

5 Conclusion

This paper presented an enhanced deep learning-based antenna selection approach. The approach employs a convolutional neural network algorithm to select a sparse subarray given a sample covariance matrix as input. Motivated by beampattern characteristics of arrays with hole-free or near hole-free coarrays, we constrained the subarrays used to generate training target data consisting of hole-free difference coarray to achieve sparse arrays with large aperture and well-distributed sensors. It has been demonstrated through numerical examples that the proposed method yields sparser arrays with improved beampattern properties and retain hole-free or near hole-free coarrays with well-distributed sensors. Moreover, the rendered sparse arrays show enhanced DOA estimation performance comparable to that of the original large array and other well-known sparse arrays.

Abbreviations

DOA:Direction-of-arrival; DL: Deep learning; CNN: Convolutional neural network; ULA: Uniform linear array; RF: Radio-frequency; SINR: Signal-to-interference-plus-noise ratio; MSE: Mean-squared-error; PSL: Peak sidelobe levels; ML: Machine learning; ANN: Artificial neural network; SVM: Support vector machine; 1-D: One-dimensional; 2-D: Two-dimensional; CRB: Cramér-Rao bound; MUSIC: Multiple signal classification algorithm; FISTA: Fast iterative soft-thresholding algorithm; MRA: Minimum redundancy array; NA: Nested array, AWGN: Additive white Gaussian noise; KR: Khatri-Rao; PSA: PSL constrained sparse array; SNR: Signal-to-noise ratio; MC: Monte Carlo; KR-MUSIC: Khatri-Rao MUSIC; RMSE: Root-mean-square-error; ReLU: Rectified linear unit; SGD: Stochastic gradient descent

Acknowledgements

The authors are sincerely thankful to the authors of [10, 11] for sharing their sample simulation codes.

Authors' contributions

Both authors have contributed towards this work as well as in compilation of this manuscript. The author(s) read and approved the final manuscript.

Funding
This work was supported in part by Japan Society for the Promotion of Science (JSPS) Grant-in-Aid for Scientific Research no. 20K04500. The authors are sincerely grateful for their support.

Availability of data and materials
Unfortunately not available online. Kindly, contact the author for data requests.

Declarations

Ethics approval and consent to participate
Not applicable.

Consent for publication
Not applicable.

Competing interests
The authors declare that they have no competing interests.

Received: 16 April 2020 Accepted: 6 April 2021
Published online: 26 April 2021

References

1. T. E. Tuncer, B. Friedlander, *Classical and modern direction of arrival estimation*. (Academic Press, Burlington, 2009)
2. H. L. Van Trees, *Optimum array processing, detection, estimation and modulation part IV*. (Wiley, New York, 2002)
3. S. Theodoridis, R. Chellappa, *Academic Press Library in Signal Processing 3 Array and Statistical Signal Processing*. (Academic Press, Inc., Orlando, FL, USA, 2013)
4. S. Joshi, S. Boyd, Sensor selection via convex optimization. IEEE Trans. Sig. Process. **57**(2), 451–462 (2009)
5. E. Tohidi, M. Coutino, S. P. Chepuri, H. Behroozi, M. M. Nayebi, G. Leus, Sparse antenna and pulse placement for colocated MIMO radar. IEEE Trans. Sig. Process. **67**(3), 579–593 (2019)
6. K. V. Mishra, Y. C. Eldar, E. Shoshan, M. Namer, M. Meltsin, A cognitive sub-Nyquist MIMO radar prototype. IEEE Trans. Aerosp. Electron. Syst. **56**(2), 937–955 (2020)
7. J. F. Hopperstad, S. Holm, in *Proc. of 3rd IEEE Nordic Signal Processing Symposium (NORSIG'98)*, The coarray of sparse arrays with minimum sidelobe level (International Speech Communication Association (ISCA), Denmark, 1998), pp. 137–140. https://www.isca-speech.org/archive/norsig_98/nos8_137.html
8. X. Wang, E. A. Aboutanios, M. G. Amin, Adaptive array thinning for enhanced DOA estimation. IEEE Sig. Process. Lett. **22**(7), 799–803 (2015)
9. X. Wang, P. Wang, X. Wang, in *Proc. of IEEE International Conference on Acoustics, Speech and Signal Processing (ICASSP)*, Adaptive sparse array reconfiguration based on machine learning algorithms, (Calgary, 2018), pp. 1159–1163
10. A. M. Elbir, K. V. Mishra, Y. C. Eldar, Cognitive radar antenna selection via deep learning. IET Radar Sonar Navig. **13**(6), 871–880 (2019)
11. A. M. Elbir, S. Mulleti, R. Cohen, R. Fu, Y. C. Eldar, in *Proc. of IEEE International Conference on Sampling Theory and Application*, Deep-sparse array cognitive radar (IEEE, Bordeaux, 2019), pp. 1–5
12. A. Beck, M. Teboulle, A full iterative shrinkage-thresholding algorithm for linear inverse patterns. SIAM J. Imaging Sci. **2**(1), 183–202 (2009)
13. R. Schimdt, Multiple emitter location of signal parameter estimation. IEEE Trans. Antennas Propag. **34**(3), 2763–280 (1986)
14. P. Stoica, A. Nehorai, MUSIC, maximum likelihood, and Cramer-Rao bound. IEEE Trans. Acoust. Speech Sig. Process. **37**(5), 720–741 (1989)
15. P. Stoica, A. Nehorai, MUSIC, maximum likelihood, and Cramer-Rao bound: further results and comparisons. IEEE Trans. Acoust. Speech Sig. Process. **38**(12), 2140–2150 (1990)
16. P. Stoica, A. Nehorai, Performance study of conditional and unconditional direction-of-arrival estimation. IEEE Trans. Acoust. Speech Sig. Process. **38**(10), 1783–1795 (1990)
17. C. Liu, P. P. Vaidyanathan, Remarks on the spatial smoothing step in coarray MUSIC. IEEE Sig. Process. Lett. **22**(9), 1438–1442 (2015)
18. P. Pal, P. P. Vaidyanathan, Nested arrays: a novel approach to array processing with enhanced degrees of freedom. IEEE Trans. Sig. Process. **58**(8), 4167–4181 (2010)
19. C. Liu, P. P. Vaidyanathan, Robustness of difference coarrays of sparse arrays to sensor failures–part I: a theory motivated by coarray MUSIC. IEEE Trans. Sig. Process. **67**(12), 3213–3226 (2019)
20. C. Liu, P. P. Vaidyanathan, Robustness of difference coarrays of sparse arrays to sensor failures–part II: array geometries. IEEE Trans. Sig. Process. **67**(12), 3227–3242 (2019)
21. A. Moffet, Minimum-redundancy linear arrays. IEEE Trans. Antennas Propag. **16**(2), 172–175 (1968)
22. A. M. Elbir, K. V. Mishra, Sparse array selection across arbitrary sensor geometries with deep transfer learning. IEEE Trans. Cogn. Commun. Netw. **7**(1), 255–264 (2021)

Publisher's Note